Cloud Macro- and Microphysical Properties Derived from GOES over the ARM SGP Domain

P. Minnis, W. L. Smith, Jr., and D. F. Young
NASA Langley Research Center
Hampton, Virginia

p.minnis@larc.nasa.gov
757-864-5671

Abstract
Proceedings of 11th ARM Science Team Meeting
Atlanta, Georgia
March 19-23, 2001

Cloud Macro- and Microphysical Properties Derived from GOES over the ARM SGP Domain

P. Minnis, W. L. Smith, Jr., and D. F. Young
NASA Langley Research Center
Hampton, Virginia

p.minnis@larc.nasa.gov
757-864-5671

Introduction

Cloud macrophysical properties like fractional coverage and height z_c and microphysical parameters such as cloud liquid water path *LWP*, effective droplet radius r_e, and cloud phase, are key factors affecting both the radiation budget and the hydrological cycle. Satellite data have been used to complement surface observations from ARM by providing additional spatial coverage and top-of-atmosphere boundary conditions of these key parameters. Since 1994, the Geostationary Operational Environmental Satellite (GOES) has been used for deriving at each half-hour over the ARM SGP domain: cloud amounts, altitudes, temperatures, and optical depths t as well as broadband shortwave (SW) albedo and outgoing longwave radiation (*OLR*) at the top of the atmosphere (see *Khaiyer et al. [2001]* for summary). A new operational algorithm has been implemented to increase the number of value-added products to include cloud particle phase and effective size (r_e or effective ice diameter D_e) as well as *LWP* and ice water path *IWP*. Similar analyses have been performed on the data from the Visible Infrared Scanner (VIRS) on the Tropical Rainfall Measuring Mission (TRMM) satellite as part of the Clouds and Earth's Radiant Energy System (CERES) project. This larger suite of cloud properties will enhance our knowledge of cloud processes and further constrain the mesoscale and single column models using ARM data as a validation/initialization resource. This paper presents the results of applying this new algorithm to GOES-8 data taken during 1998 and 2000. The global VIRS results are compared to the GOES SGP results to provide appropriate context and to test consistency.

Data

Half-hourly, 4-km GOES-8 imager pixels with reflectances at 0.65 (VIS) and brightness temperatures T at 3.9 (SI), 10.8 (IR), and 12.0 μm (WS) were analyzed over a domain covering the area between 32°N and 42°N and between 91°W and 105°W. The entire domain was used for data taken during the Spring 2000 Intensive Observing Period (IOP) from March 1 through April 6, 2000. Data for a 0.3° box centered on the ARM Southern Great Plains (SGP) central facility (SCF) were analyzed for daylight, defined as solar zenith angle SZA < 78°, between January 1 and December 31, 1998. The GOES-8 VIS data were calibrated using coincident VIRS data (*Minnis et al. 2001*).

CERES Edition-1 average cloud properties derived from 2-km VIRS pixels were computed for a 0.3° box centered over the SCF. The VIRS data were taken at different times of day that changed each day because of TRMM's precessing orbit. The CERES analyses use channels similar to those on GOES-8 and covered the first 8 months of 1998. For more details, see http://eosweb.larc.nasa.gov/PRODOCS/ceres/SSF/Quality_Summaries/CER_SSF_TRMM_Edition1.html.

Temperature and humidity profiles from the Rapid-Update Cycle (RUC; *Benjamin et al. 1994*) analyses were used to correct the radiances for atmospheric absorption and to provide an initial guess at surface skin temperature for the GOES-8 analyses. The VIRS analyses used European Center for Medium-range Weather Forecasting (ECMWF) analyses for the same purposes.

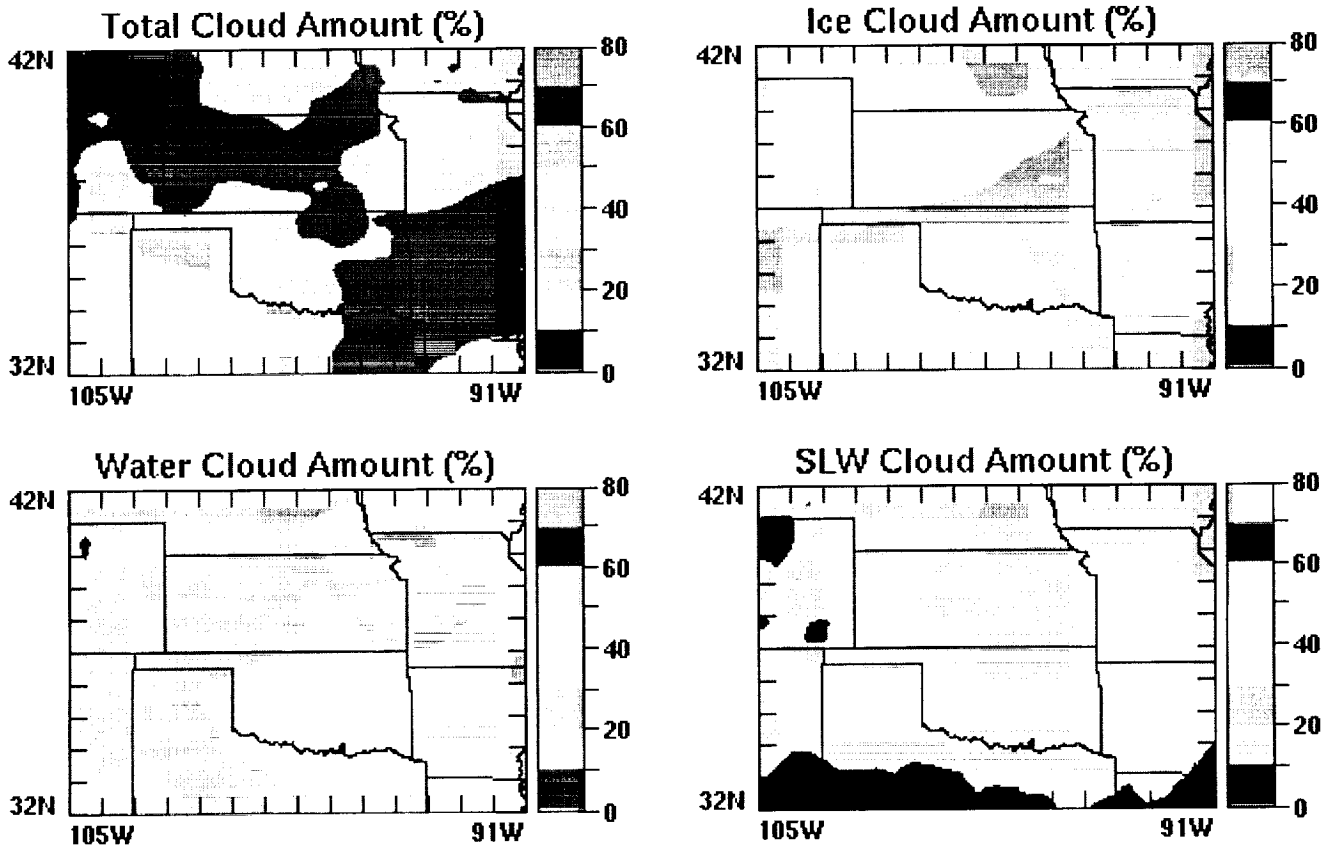

Fig. 1. Mean daytime cloud amounts from GOES-8 during Spring 2000 IOP.

Methodology

A 4-channel update, the Visible Infrared Solar-infrared Split-window Technique (VISST), of the multispectral method described by *Minnis et al. (1995)* using the models of *Minnis et al. (1998)* were used together with the technique of *Minnis and Smith (1998)* to derive cloud fraction, height, temperature, r_e, D_e, *LWP*, and *IWP* and SW albedo and *OLR* for each GOES-8 pixel. The combination of these parameters can also be used to determine which clouds are composed of supercooled liquid water SLW. Surface emissivities were estimated for each thermal channel using an updated version of the method described by *Smith et al. (1999)*. The values of r_e, D_e, t, and water paths were found to agree

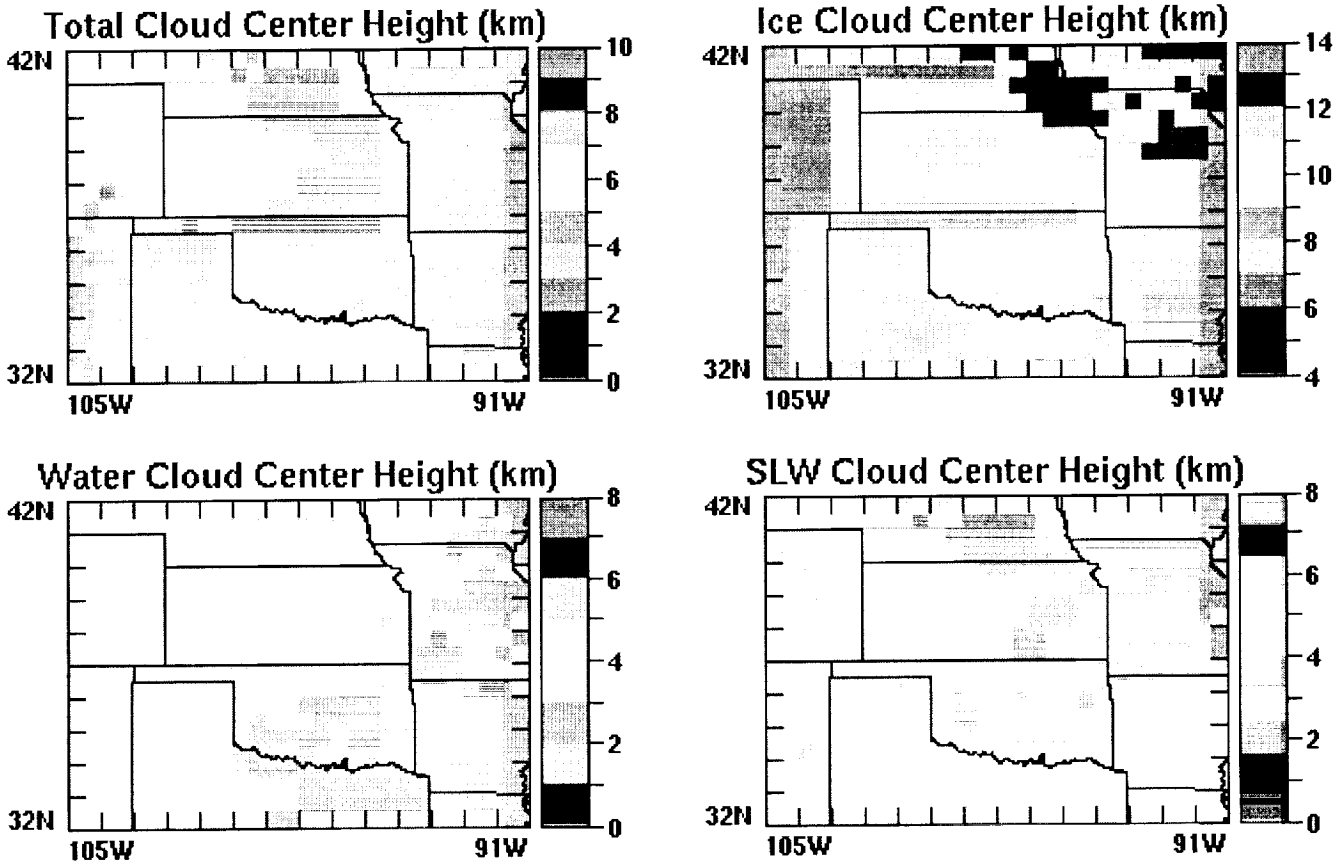

Fig. 2. Same as Fig. 1, except for mean cloud heights.

well with both in situ (e.g., *Young et al. 1998*) and radar-radiometer retrievals (*Mace et al. 1998*; *Dong et al. 2001*) for single-layer clouds. Multilayered clouds can produce significant errors, especially in the derived particle sizes (e.g., *Kawamoto et al. 2001*).

Results

Spring 2001 IOP

The mean gridded cloud amounts for the Spring 2001 IOP in Fig. 1 show total cloud amounts ranging from 30% in the southwestern corner of the domain values as great as 69% in the northwestern corner. The areas with the greatest cloud amounts are dominated by ice clouds, while liquid water clouds are more prevalent elsewhere. A substantial portion of the liquid water clouds consist of SLW, at least in the part of the cloud viewed by the satellite. The mean cloud heights (Fig. 2) reflect the relative distribution of ice and water with the greatest heights occurring in the northwestern part of the domain. In this case, the cloud center height refers to height of the effective radiating center of the cloud. For liquid-water clouds, this center is very close to the cloud top, while for ice clouds it may be 1-2 km below the top because of the relatively small optical depths in the tops of physically thick ice clouds. The mean ice cloud heights range from 5.5 to 8 km, while the liquid water cloud heights vary from 2 to 5 km. The SLW clouds are typically at higher altitudes, 3.5 to 5 km, than the average water cloud. This range of mean total cloud heights is typical for this domain although the pattern is not necessarily typical. *Khaiyer et al. (2001)* provide more details of the climatological values of these properties.

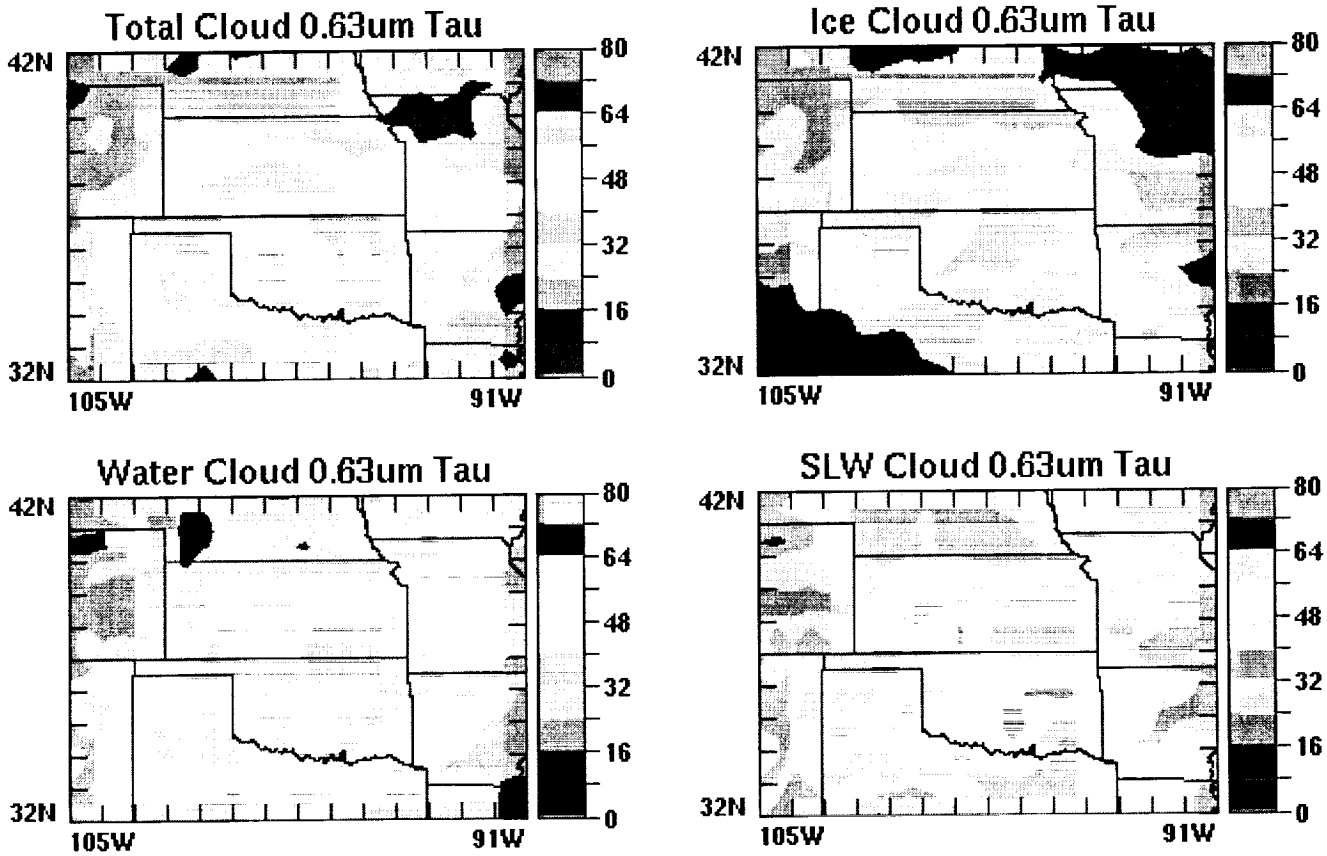

Fig. 3. Same as Fig. 1, except for cloud optical depths.

Mean cloud optical depths (OD) are greatest over Oklahoma during the IOP with maximum values near 45 (Fig. 3). Several cyclones developed and stalled over the state during the period resulting in the patterns seen here. The largest mean ODs were found in the SLW clouds. Larger instantaneous values probably occurred for the ice clouds. Mean ice cloud optical depths fell below 8 in the southwestern corner of the domain. Figure 4 shows the mean values of r_e for all liquid water clouds, SLW clouds only, and all water clouds that were observed in a grid box free from any pixels identified as ice clouds. Mean LWP values are also provided. For all cases, r_e varies from 10 to 15 μm over the domain. Similar values are observed for the SLW clouds. However, if the ice-contaminated boxes are removed, the range of r_e is reduced to values between 8 and 12 μm. The apparent 2-μm difference in mean r_e between all cases and the ice-free cases is probably due to multilayered or mixed-phase clouds which tend to increase the derived particle size (e.g., *Kawamoto et al. 2001*). LWP varies from 100 to 350 gm^{-2} with the maximum values occurring in the same locations as the peak ODs. The mean ODs were unusually large over Oklahoma during the 2001 IOP.

1998 SCF Averages

The plots in this section denote the seasons as numerals with 1 and 4 representing winter and fall, respectively. Mean cloud amount over the SCF in Fig. 5 shows that the maximum coverage occurred during the fall in 1998 with a minimum during the summer. The average total cloud fraction for the year was 50% composed of roughly 40% ice and 60% water. Mean total cloud heights (not shown) were greatest during summer at 5.6 km and lowest during autumn at 4.4 km. Total optical depths were

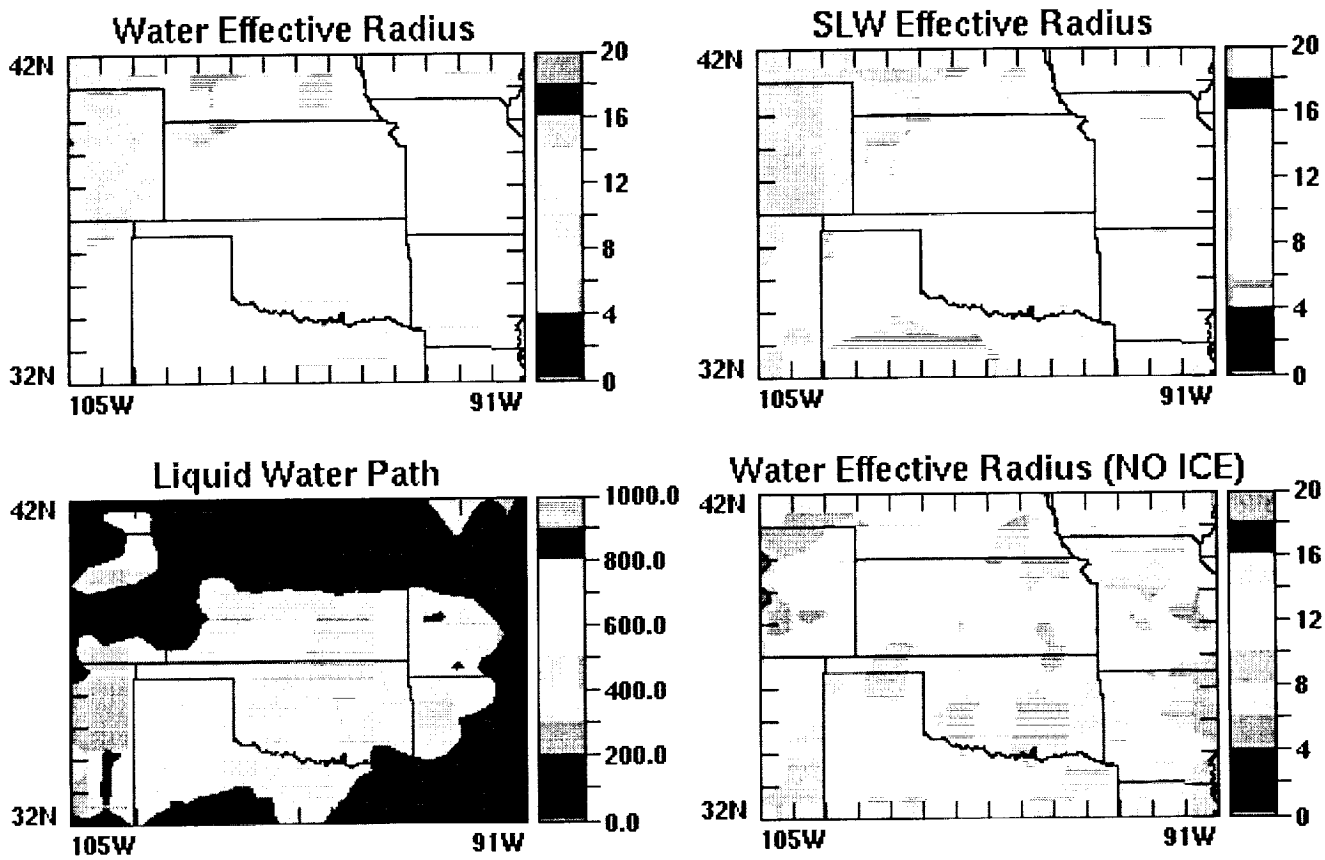

Fig. 4. Same as Fig. 1, except for cloud water droplet sizes and liquid water path.

greatest during winter and least during the summer, although the ice cloud OD was least during fall. Ice cloud OD was smaller than the water cloud value only during fall. Cirrus, defined as ice clouds having $t < 4$, coverage (not shown) was greatest during winter and fall. Mean cirrus heights varied from 6 km in winter to 8 km during the summer. Many cirrus overlapped lower clouds and, therefore, were not identified as such because the total OD exceeded 4 for those cases.

The mean cloud effective particle sizes (Fig. 6) show a slight seasonal variation with minima in both r_e and D_e during the summer. The average annual values for these parameters are 10.8 and 56 μm, respectively. These values are typical of the global averages derived over land areas by CERES from VIRS data. Consistent with the variations in OD and particle size, the LWP and IWP values peak during winter and bottom out during the summer. The large mean values of IWP are dominated by the passage of deep cyclonic systems and convective storms.

VIRS Comparisons

In addition to comparisons with the reference datasets derived from in situ measurements and active remote sensors noted earlier, it is possible to assess an uncertainty in the satellite-derived cloud properties using comparisons with similar retrievals taken at other viewing angles. VIRS data are valuable for such comparisons because of the changing local time coverage. GOES-8 observes the SCF at constant viewing zenith angle (VZA) of 53°, while VIRS has a VZA varying from 38° to 48° with azimuth angles that differ from GOES-8. The mean matched cloud fractions from GOES-8 for 1998 are

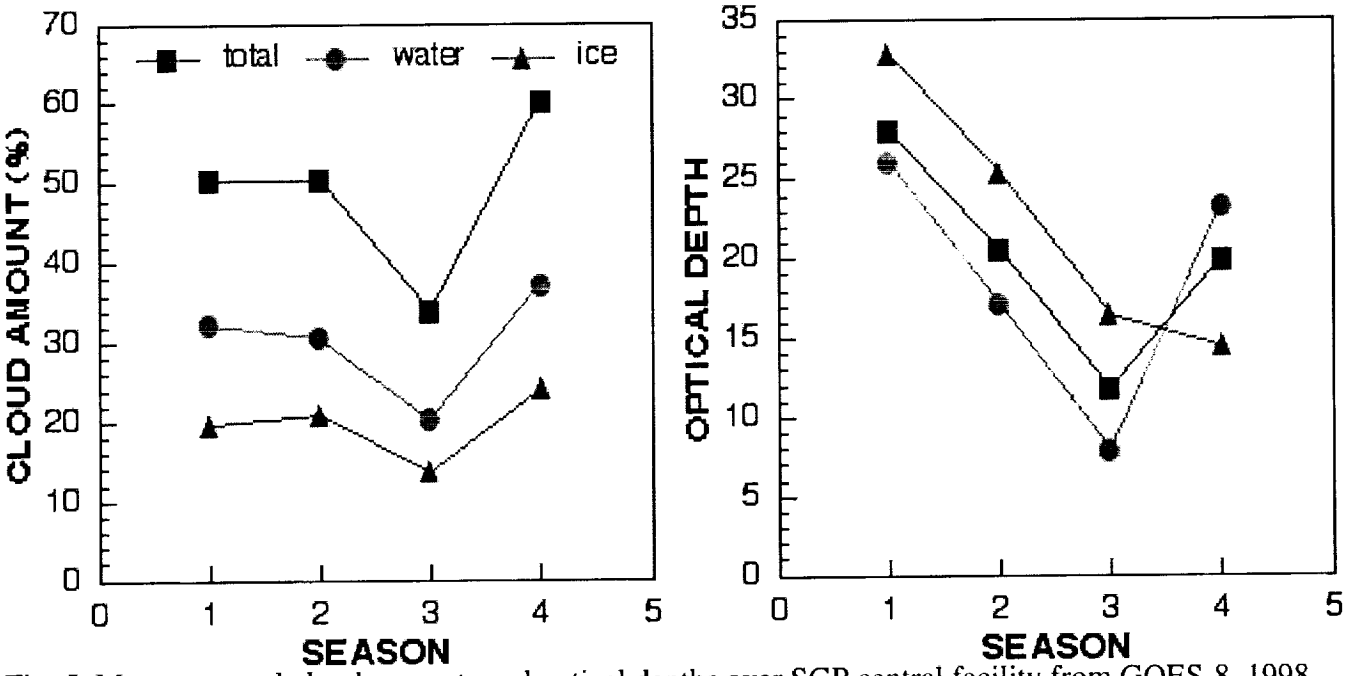

Fig. 5. Mean seasonal cloud amounts and optical depths over SGP central facility from GOES-8, 1998.

4% greater than those from VIRS with an RMS difference of 20%. The magnitude of these differences is expected given the different VZAs and pixel resolutions.

Figure 7 shows the scatterplots of cloud heights derived from the two satellite instruments for mostly overcast and broken cloud cases separately. For the overcast (CLD > 95%) cases, the mean difference is only 0.2 km with a 0.8 km standard deviation (std). When only broken cloud cases are considered, however, the mean GOES-8 heights are 0.8 km higher than their VIRS counterparts with much greater

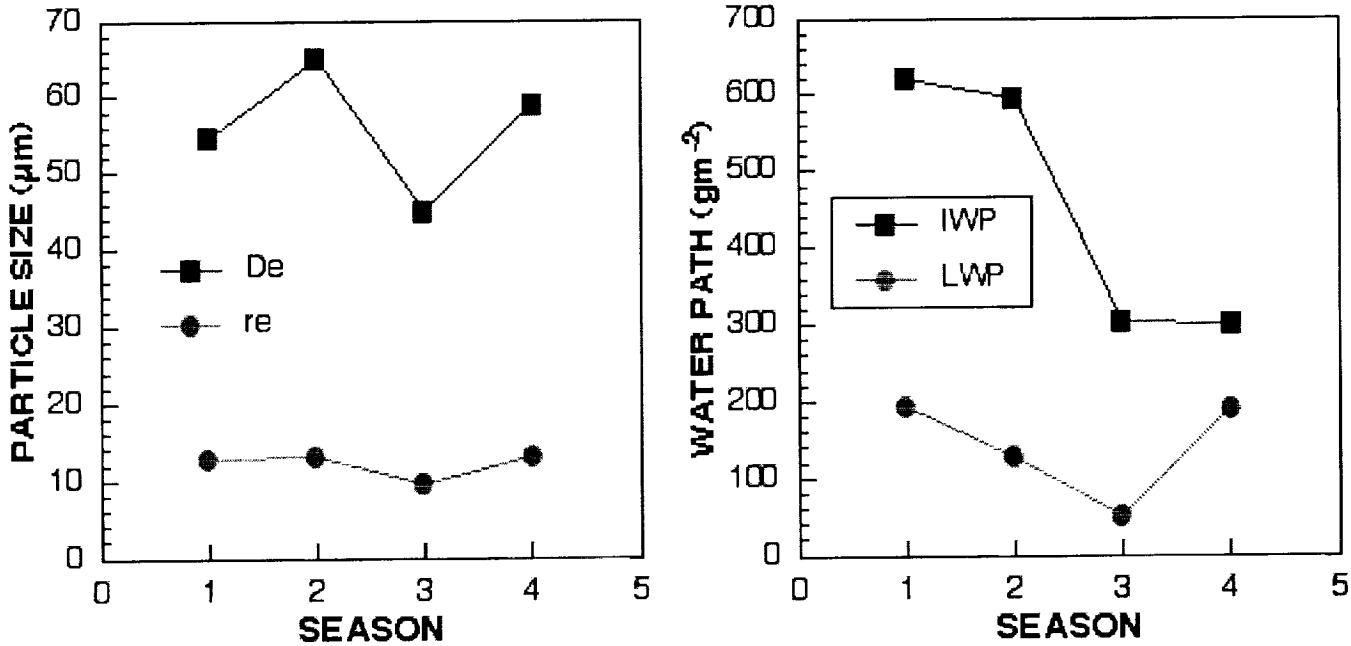

Fig. 6. Same as Fig. 5, except for cloud particle size and water path.

References

Benjamin, S. G., K. J. Brundage, and L. L. Morone, 1994: The Rapid Update Cycle. Part I: Analysis/model description. Technical Procedures Bulletin No. 416, NOAA/NWS, 16 pp.

Dong, X, P. Minnis, W. L. Smith,. Jr, and G. G. Mace, 2001: Comparison of boundary layer cloud properties using surface and GOES measurements at the ARM SGP site. *Proc. 11th ARM Science Team Meeting*, Atlanta, GA, March 19-23.

Kawamoto, K, P. Minnis, and W. L. Smith, Jr., 2001: Cloud overlapping detection algorithm using solar and IR wavelengths with GOES data over the ARM/SGP site. *Proc. 11th ARM Science Team Meeting*, Atlanta, GA, March 19-23.

Khaiyer, M. M., W. L. Smith Jr., A. D. Rapp,, M. L. Nordeen, and P. Minnis, 2001: A three-year climatology of cloud and radiative properties derived from GOES-8 data over the Southern Great Plains. *Proc. 11th ARM Science Team Meeting*, Atlanta, GA, March 19-23.

Mace, G. G., T. P. Ackerman, P. Minnis, and D. F. Young, 1998: Cirrus layer microphysical properties derived from surface-based millimeter radar and infrared interferometer data. *J. Geophys. Res.*, **103**, 23,207-23,216.

Minnis, P., D. P. Garber, D. F. Young, R. F. Arduini, and Y. Takano, 1998.: Parameterization of reflectance and effective emittance for satellite remote sensing of cloud properties. *J. Atmos. Sci.*, **55**, 3313-3339.

Minnis, P., D. P. Kratz, J. A. Coakley, Jr., M. D. King, D. Garber, P. Heck, S. Mayor, D. F. Young, and R. Arduini, 1995: Cloud Optical Property Retrieval (Subsystem 4.3). "Clouds and the Earth's Radiant Energy System (CERES) Algorithm Theoretical Basis Document, Volume III: Cloud Analyses and Radiance Inversions (Subsystem 4)", *NASA RP 1376 Vol. 3*, edited by CERES Science Team, pp. 135-176.

Minnis, P., L. Nguyen, D. R. Doelling, D. F. Young, and W. F. Miller, 2001: Rapid calibration of Operational and research meteorological satellite imagers, Part I: Use of the TRMM VIRS or ERS-2 ATSR-2 as a Reference. Submitted to *J. Atmos. Oceanic Technol.*

Minnis, P. and W. L. Smith, Jr., 1998: Cloud and radiative fields derived from GOES-8 during SUCCESS and the ARM-UAV Spring 1996 Flight Series. *Geophys. Res. Lett.*, **25**, 1113-1116.

Smith, W. L., Jr., P. Minnis, D. F. Young, and Y. Chen, 1999: Satellite-derived surface emissivity for ARM and CERES. *Proc. AMS 10th Conf. Atmos. Rad.*, Madison, WI, June 28 – July 2, 410-413.

Young, D. F., P. Minnis, D. Baumgardner, and H. Gerber, 1998: Comparison of in situ and satellite-derived cloud properties during SUCCESS. *Geophys. Res. Lett.*, **25**, 1125-1128.